Improved Exponential Time Series Approximation of Unsteady Aerodynamic Operators

Lee D. Peterson* and Edward F. Crawley†
Massachusetts Institute of Technology, Cambridge, Massachusetts

A procedure has been developed for approximating unsteady aerodynamic operators as truncated exponential series in the time domain. The approximation is accomplished using a least squares minimization fit to aerodynamic data in the frequency domain. The procedure extends previous methods by including the pole locations as unknown parameters of the least squares minimization. In addition, the error associated with both the real and imaginary parts of the Fourier transform of the approximation is minimized. A Newton-Raphson search algorithm is used to find the minimum of the weighted square error in the parameter space of the approximation while constraining the poles to be in the left half-plane. By freely varying the poles of the approximation during the numerical least squares minimization, the representation of the unsteady aerodynamics is improved and is comparable to existing higher-order Pade approximations. Hence, the method offers the aeroelastic designer a more direct method of finding approximate aerodynamic states. However, because the minima of the square error in the cost function found are not necessarily global and depend on the number of poles in the approximation, the initial trial minimum, and the details of the cost minimization algorithm, the poles found in the search do not necessarily correspond to the theoretical poles of the aerodynamic transfer function. Example exponential time series approximations of the Theodorsen function are presented and compared with a Pade approximation and other exponential time series approximations.

Nomenclature

A = curvature matrix of the cost function J
$\underline{A}$ = true aerodynamic impulse response spectrum
$\underline{A}'$ = approximate aerodynamic impulse response spectrum
$\underline{a}$ = coefficient defined in Eq. (14)
a_n = coefficients of the approximation
b_n = pole locations of the approximation
c = cost minimization step length
C = Theodorsen circulation function
d = cost minimization search direction vector
F = real part of $\underline{A}$
F' = real part of $\underline{A}'$
g = gradient of the cost function J
G = imaginary part of $\underline{A}$
G' = imaginary part of $\underline{A}'$
J = weighted square error cost function
k = reduced frequency
k_{max} = frequency corresponding to the peak in $|G|$
M = number of data points to be fitted
N = number of terms in the series
t = nondimensional time
s = Laplace domain variable
x = parameter vector of the coefficients and poles
α_m = weighting factors for the real part of the approximation error
β_m = weighting factors for the imaginary part of the approximation error
ϕ = true step response
ϕ' = approximate step response

Presented as Paper 85-0663 at the AIAA/ASME/ASCE/AHS 26th Structures, Sturctural Dynamics and Materials Conference, Orlando, FL, April 15-17, 1985; received Sept. 8, 1986; revision received June 5, 1987.

*Research Assistant. Member AIAA.
†Associate Professor of Aeronautics and Astronautics. Member AIAA.

Introduction

UNSTEADY aeroelastic analysis relies on an accurate representation of the generalized aerodynamic forces in a convenient computational form. The lift and moment aerodynamic operators for the arbitrary translation and pitching of a vibrating wing are most often determined in the frequency domain, even though the aeroelastic analysis usually must be carried out in the Laplace domain (for flutter or control analysis) or in the time domain (for gust response or for simulation of the aircraft motion).[1-5] Even for the few cases in which analytic expressions for aerodynamic operators are known in the frequency domain, exact conversion to the time domain is difficult or awkward. For the case of transfer functions determined at discrete frequencies by computational or experimental methods, analytic transformation to the time domain is impossible. It is, therefore, necessary to perform the conversion using an assumed approximate form that has both a convenient time and Laplace representation. Additionally, the approximation must be accomplished using as low an order as possible because, in general, each additional term in an approximate aerodynamic form adds a state to the aerodynamic operator and, hence, adds a state to the aeroelastic formulation.

The most commonly assumed approximate forms of unsteady aerodynamic operators fall into two categories: Pade approximations, for which the Laplace domain aerodynamic transfer functions are assumed to be the ratio of finite-degree polynomials in the Laplace domain variable, and exponential time series approximations, for which the time domain aerodynamic transfer functions are assumed to be a finite series of lag exponentials. Although the two representations are theoretically identical, they differ in their derivation.

The Pade approximation has probably been more widely used, however, because the minimum of its approximation square error cost function can be analytically found in some simple cases. Vepa[6] developed such a Pade approximation procedure for finding unsteady aerodynamic operators. However, as pointed out by Dunn,[7] an application of the analytical Pade approximation to complicated systems, such as those having more than two flexible modes or having an

imprecise aerodynamic description, can result in an unstable representation. For this reason, Dunn has developed a Pade approximation procedure that insures stability by constraining the poles of the aerodynamic transfer function to be negative. That procedure used a constrained numerical search to identify the Pade coefficients.

The exponential time series representation, whose parameters include the aerodynamic poles as the inverse of the time constants and the coefficients of the corresponding terms, can be superior and preferable to Pade approximations in aeroelastic analysis, as indicated by Dowell.[8] The aerodynamic states—the poles of the aerodynamic transfer function—are explicit parameters of the exponential time series approximation, but can be determined only implicitly from the parameters of a Pade approximation. In addition, the least squares derivation of a Pade approximation gives undue numerical weighting to data at higher reduced frequencies.

The exponential time series representations result in a square error cost function that is quadratic in the coefficients, but not in the poles. As a consequence, the minimum error approximation must be found by a numerical search if both the poles and the coefficients of the series are parameters. In the past, this difficulty has been avoided by choosing pole locations for the exponential representation *a priori* and finding the coefficients by analytically minimizing the resulting square error cost function. Desmarais[11] used the calculated poles of the continued fraction representation of the Theodorsen function. Dowell[8] generalized this procedure for an arbitrary aerodynamic transfer function for which Fourier domain data are available at discrete frequencies. The poles of the approximation were placed at or near the reduced frequencies corresponding to peaks in the imaginary part of the transfer function. The coefficients of the approximation were then chosen by a constrained minimization search for the least square error in the imaginary part of the approximation. The sum of the coefficients of the approximation, equal to the high-frequency asymptote on the real part of the approximation, was numerically constrained to be the same as the corresponding high-frequency asymptote on the aerodynamic data. Only by carefully choosing the poles of the approximation could this yield a comparable approximation to that of the Pade approximation.

As with a Pade approximation, a numerical minimization will be necessary to formulate an exponential time series approximation for a complex system. Heuristic choices of the pole locations are not available and, hence, the poles of the aerodynamic transfer function are free parameters of the approximation. Both Refs. 8 and 11 suggested that the inclusion of pole locations as free parameters in the approximation would lead to better approximations and, indeed, as shown in this paper for a simple approximation to the Theodorsen function, this is the case. The algorithm developed here includes in the cost function both the real and imaginary parts of the aerodynamic transfer function. A Newton-Raphson nonlinear programming algorithm minimizes the cost function in the combined parameter space of the coefficients and poles subject to the inequality constraint that the poles lie in the left half-plane.

The resulting procedure is compared with the Pade approximation of Vepa[6] for the Theodorsen function.[9] In addition, the effect of the order of the approximation (the number of terms in the exponential series) is examined. A third-order exponential approximation found using this procedure will be shown to more closely approximate the Theodorsen function than a fourth-order Pade approximation of Vepa.[6]

Unlike the algorithm of Ref. 8, however, the equality constraint on the sum of the coefficients is not imposed because the high-frequency asymptote for experimental data is not necessarily known. In contrast with the Pade approximation method in Ref. 7, the stability constraint is imposed explicitly on the parameters of the approximation, while for the Pade approximation the poles of the denominator polynomial must first be found before the constraint can be imposed. This greatly complicates the application of a numerical search routine to Pade approximations and is another advantage of exponential time series.

This method was applied in Ref. 5 for determining the impulse response of the pressure distribution for a three-dimensional wing. The doublet-lattice method was used to provide values of the pressure transfer function at discrete values of reduced frequency. By applying the numerical search algorithm individually to each entry in the doublet-lattice aerodynamic operator, this algorithm yielded a complete time domain representation of the wing pressure response.

Cost Function Derivation

The approximation algorithm will be developed in two parts. First, the exponential representation and the corresponding quadratic cost function are formulated. Then, the cost function minimization algorithm used to obtain the results in this paper is described.

Following Dowell's description in Ref. 8, the aerodynamic operator is assumed to be represented by an impulse response spectrum $\underline{A}(k)$, which is available at M values of k, the reduced frequency, in the form

$$\underline{A}(k_m) = F(k_m) + iG(k_m), \quad m = 1,2...M \tag{1}$$

where $\underline{A}(k_m)$ is the complex spectrum of the aerodynamic impulse response and $F(k_m)$ and $G(k_m)$ its real and imaginary parts, respectively. These values might be obtained from analysis, computation, or experiment. In general, $\underline{A}(k)$ can be one entry in a large aerodynamic operator matrix for a lifting surface. The values of the reduced frequency k_m are not necessarily evenly spaced or ordered and may themselves be experimentally observed. The impulse response at zero frequency $F(0)$ must be known and is designated a_0.

The exact time domain step response $\phi(t)$ and the exact impulse response $A(t)$ are most conveniently related through their Fourier transforms[1]

$$\underline{A}(k) = ik\underline{\phi}(k) \tag{2}$$

An approximate step response $\phi'(t)$ is assumed to be of the form

$$\phi'(t) = \sum_{n=0}^{N} a_n e^{b_n t} \tag{3}$$

where N is the number of aerodynamic states included in the approximation, t the nondimensional time (dimensional time times the free stream air velocity divided by the wing semichord), and a_n and b_n the unknown parameters of the approximation, the coefficients and pole locations, respectively. Only real b_n are considered; that is, only first-order lags in the aerodynamics are allowed. Complex pole pairs, which would correspond to second-order resonances in the aerodynamics, are usually excluded. This choice has been justified by experimental observation and, most recently, by analysis.[8,11] In particular, the analysis of Ref. 11 observed that the Theodorsen circulation function, although it has no exact analytic poles, may be expressed as a truncated approximation with poles along the negative real axis, which is the branch cut of the Theodorsen function. As the approximation improves, the poles will become infinitely dense. The first pole b_0 is constrained to be zero, so that the first coefficient of the series is the known low-frequency asymptote a_0. The remaining poles b_n $(n = 1,2,...N)$ are restricted to be less than zero. Otherwise, the approximation would represent an unbounded growing aerodynamic force. If these a_n

and b_n are chosen so that the spectrum of ϕ' closely fits the known spectrum of the aerodynamic transfer function, an approximate aerodynamic transfer function in the time domain would be given by Eq. (3) and the Laplace domain representation could be readily derived. From Eqs. (2) and (3), the Fourier transform for the impulse response of the approximation series representing the step response is

$$\underline{A}'(k) = ik\underline{\phi}'(k) = \sum_{n=0}^{N} \frac{ika_n}{-b_n + ik}$$

$$= a_0 + \sum_{n=1}^{N} \frac{ika_n}{-b_n + ik} \tag{4}$$

since b_0 is identically zero. The corresponding real and imaginary parts of the approximation are

$$F'(k) = a_0 + \sum_{n=0}^{N} \frac{a_n k^2}{b_n{}^2 + k^2} \tag{5}$$

$$G'(k) = \sum_{n=1}^{N} \frac{-a_n b_n k}{b_n{}^2 + k^2} \tag{6}$$

These series have been guaranteed to satisfy the low-frequency asymptotic behavior of the known aerodynamic data,

$$F'(0) = a_0$$

$$G'(0) = 0 \tag{7}$$

because of the choice of a_0 and b_0.

The $2N$-dimensional vector of the approximation parameters

$$\boldsymbol{x}^T = [a_1 a_2 a_3 \ldots a_N b_1 b_2 b_3 \ldots b_N] \tag{8}$$

must be chosen to minimize the difference between the approximations F' and G', and the exact aerodynamic data F and G, which are known at the M discrete values of k. This error is expressed mathematically by the weighted square error cost function $J(\boldsymbol{x})$:

$$J(\boldsymbol{x}) = \sum_{m=1}^{M} \{\alpha_m [F_m - F'(\boldsymbol{x}, k_m)]^2 + \beta_m [G_m - G'(\boldsymbol{x}, k_m)]^2\}$$

$$= \sum_{m=1}^{M} \left[\alpha_m \left(F_m - a_0 - \sum_{n=1}^{N} \frac{a_n k_m{}^2}{b_n{}^2 + k_m{}^2}\right)^2 + \beta_m \left(G_m + \sum_{n=1}^{N} \frac{a_n b_n k_m{}^2}{b_n{}^2 + k_m{}^2}\right)^2\right] \tag{9}$$

where α_m and β_m are weighting factors. The minimum of J in the $\boldsymbol{x}$ space will indicate the best approximation to the true transfer function evaluated at a finite number of reduced frequencies.

Cost Minimization Algorithm

The approximation procedure centers on the nonlinear programming problem of finding a minimum of $J(\boldsymbol{x})$ in the parameter space $\boldsymbol{x}$, subject to the constraint that the poles of the approximation b_n are less than zero. A standard Newton-Raphson search method will be used to find this minimum. In this recursive search procedure, an initial point $\boldsymbol{x}_0$ satisfying the constraints is chosen, and second-order steps in the parameter space are made in the direction of locally decreasing cost to form the recursion sequence,

$$\boldsymbol{x}_{i+1} = \boldsymbol{x}_i + c_i \boldsymbol{d}_i, \quad i = 0,1,2\ldots \tag{10}$$

where c_i is a calculated step length and $\boldsymbol{d}_i$ the $2N$-dimensional step direction vector calculated using the approximation $\boldsymbol{x}_i$. Under some circumstances, the constraints require that the search direction be modified to avoid violating the constraints. Figure 1 is a graphic representation of a typical minimization search.

The starting point $\boldsymbol{x}_0$ is chosen by a procedure similar to the procedure of Ref. 8. Consider the single-term exponential approximation to the step response, ae^{bt}. The corresponding imaginary part of the approximate impulse response G' is

$$G'(k) = -ak^2/(b^2 + k^2) \tag{11}$$

The absolute value of this function has a maximum at

$$k = k_{\max} = -b \tag{12}$$

and the value at that peak is $-a/2$. This information is used to set the values of the initial approximation $\boldsymbol{x}_0$. The first pole b_1 is set to the value $-k_{\max}$ corresponding to the peak value of $|G(k_m)|$, the imaginary part of the aerodynamic frequency data. The remaining b_n are equally distributed between 0 and $-k_M$, the largest discrete frequency at which data are provided. The initial a_n are likewise based on F and G. The first coefficient a_1 is set to twice the value of $G(k_{\max})$. The remaining a_n are chosen so that the sum of all the a_n equals the high-frequency asymptote of $F(k)$, approximated in the data by $F(k_M)$. The $a_n (n = 2,3,\ldots N)$ for the starting point, then, are assumed to form a geometric series

$$a_{j+2} = \underline{a}(-\tfrac{1}{2})^j, \quad j = 0,1,2,\ldots N-2 \tag{13}$$

where

$$\underline{a} = [F(k_M) - a_0 - a_1] \frac{3/2}{1 - (-\tfrac{1}{2})^{N-1}} \tag{14}$$

This can be shown to satisfy the relation

$$\sum_{n=0}^{N} a_n = F(k_M) \tag{15}$$

from the rules for the evaluation of a partial sum.[12] Thus, the initial approximation satisfies the high-frequency asymptote constraint imposed on every approximation in Dowell's method.[8]

The principal search direction is the Newton-Raphson step

$$\boldsymbol{d} = -\boldsymbol{A}^{-1}\boldsymbol{g} \tag{16}$$

in which $\boldsymbol{g}$ is the gradient vector of the cost function $\partial J/\partial \boldsymbol{x}$, and $\boldsymbol{A}$ the Hessian (the second derivative matrix) of the cost function $\partial^2 J/\partial \boldsymbol{x}^2$. When the cost function is quadratic, this search direction vector $\boldsymbol{d}$ will point to the exact minimum. The cost function $J(\boldsymbol{x})$, however, is not quadratic, so more than one step will be needed to find the minimum. Occasionally, the cost function will be locally convex, meaning that the Newton-Raphson step will point away from the minimum and toward the convex maximum. In such a case, a simple gradient step, although computationally less efficient, would be more appropriate:

$$\boldsymbol{d} = -\boldsymbol{g} \tag{17}$$

Local convexity is detected when the computed Newton-Raphson step points toward increasing cost. Since $-\boldsymbol{g}$ always points toward decreasing cost, the Newton-Raphson step is not chosen when the numerical projection (vector dot product) of $-\boldsymbol{A}^{-1}\boldsymbol{g}$ on $-\boldsymbol{g}$ is negative.

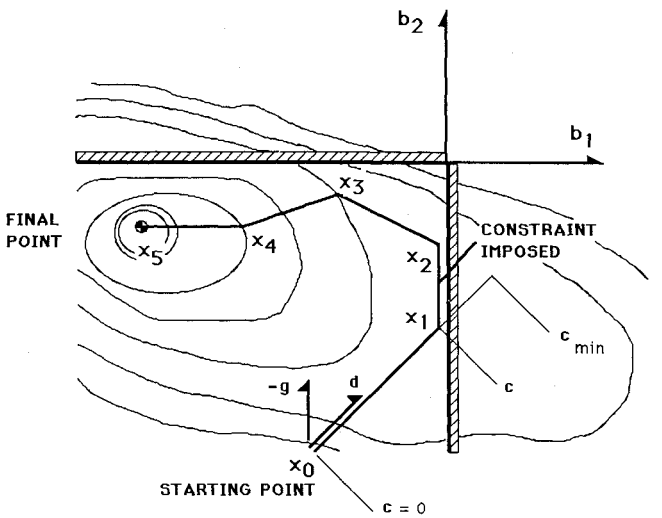

Fig. 1 Diagram for a typical parameter search for the minimum of the least squares cost function. The minimum is reached here in five steps. The constraint that the aerodynamic poles be less than zero is imposed between x_1 and x_2 by the restriction on the search direction vector d.

In evaluating the search direction vector d, the exact analytic expressions for g and A may be used. These are derived in Ref. 5 by a term-by-term differentiation of Eq. (9).

The constraints can be explicitly imposed on the search direction d because they are homogeneous in the parameter vector x. Each constraint $b_n < 0$ can be treated geometrically as a barrier to the search. As a particular b_n approaches zero and the search nears the corresponding constraint boundary, the computed component of the step vector d that moves toward the constraint barrier is set to zero. A numerical switch makes that constraint "active." Similarly, the components of the search direction vector d corresponding to any and all active constraints are set to zero, thereby moving any motion in the next step toward any of the nearby boundaries. All other components of d are unchanged. If the search ever moves to a point with any particular active constraint's component of d pointing away from its corresponding constraint boundary, the constraint is made once again inactive and its component in d is set to the computed value.

The scalar c determines the size of the step to be taken. Since the formulation of d involves a great deal of computation, c should be as large as possible for overall computational efficiency. In the search algorithm, c is chosen to be the smaller of two possible computed values: that which specifies a quadratic minimum along d and that which reaches a constraint boundary. Both may be calculated without computing g and A at intermediate points. The step length that specifies a quadratic minimum along the step direct is estimated using three evaluations of the cost J along the direct d. To do this, successive evaluations of the cost are made at equally spaced intervals along d until the cost minimum is bracketed. A parabolic fit is made to the values of J based on the last three values of c.

The iterative search process continues until the stopping criteria are satisfied. At a minimum of J, the gradient of the error function g would be identically zero, unless the minimum is on a constraint boundary, for which the component parallel to the boundary would be zero. The primary convergence test, therefore, is that the computed magnitude of g falls below a threshold, typically on the order of 10^{-5}. Other stopping criteria are also considered. If the incremental change in the cost for each step falls below a small threshold consistently for a given number of steps (typically 10), then the steps are not greatly improving the cost and the search is halted. If the first two criteria are never satisfied, the search is stopped after a specified number of steps (typically 50).

Table 1 Discrete values of the exact Theodorsen function used in the approximations

Reduced frequency, K	Real part F	Imaginary part G
0.0	1.000	0.000
0.025	0.965	−0.090
0.050	0.911	−0.132
0.1	0.846	−0.163
0.2	0.728	−0.189
0.3	0.665	−0.180
0.4	0.624	−0.166
0.5	0.603	−0.151
0.6	0.579	−0.138
0.8	0.554	−0.116
1.0	0.539	−0.100

Consider the typical search for a two-pole approximation as graphically presented in Fig. 1. The migration of the search through the b_1 and b_2 space is plotted; the a_1 and a_2 coordinates of x have not been shown. The search begins at the initial location x_0. At this point, the gradient and Hessian of the cost function are evaluated. The Newton-Raphson step is found to have a positive component along $-g$, so that it is chosen to become the step direction d. The algorithm then begins to determine the step length c. In this example, the value of c that is found would make the value of b_1 at the next point x_1 positive. The value of c used is reduced from $c_{\min}$ so that the value of b_1 at x_1 is just inside the constraint boundary. This constraint becomes active and for the next step, to x_2, the component of the search perpendicular to the constraint boundary is set to zero. At x_2 the search direction points away from the constraint boundary and the constraint is made inactive so that the b_1 component of d can be used. The procedure repeats until x_5, where the gradient calculated is very small and the search is converged.

Application of the Procedure to an Approximation of the Theodorsen Function

Two assessments of the effectiveness and value of this approximation algorithm were carried out. In the first, the sensitivity of the approximation on the number of poles N and on the initial approximation x_0 was studied by numerical examples. In the second phase, the accuracy of the approximations was compared with that of other well-known exponential time series approximations and with the Pade approximations.

As a basis for this study, an exponential time series approximation of the Theodorsen two-dimensional incompressible circulation function was sought. Table 1 shows the analytical evaluations of F and G.[9] Thirteen example approximations are presented in Table 2. In deriving all these examples, the weighting factors α_m and β_m were set to one. In order to study the effect of increasing the order of the approximation, cases 1-7 correspond to 1-7 pole approximations. The initial approximation x_0 was chosen by the method outlined in Eqs. (13-15). The effect of different initial approximations x_0 are shown in cases 8-13. Case 8 used as its initial approximation the well-known two-pole Jones approximation.[10] Cases 9 and 10 have starting points corresponding to two of Dowell's best three-pole fits.[8]. Cases 11-13 have arbitrarily chosen starting points.

Figure 2 shows the cost in the approximation [Eq. (9)] of each example as a function of the number of poles. There is general improvement in the approximation up to four poles, but little additional improvement in the approximation above four poles. In fact, case 4, a four-pole series, and case 7, a seven-pole series, have almost the same cost. Note that the five- and six-pole approximations actually have a higher cost than the four-pole case. Clearly, monotonic decrease in cost

Table 2 Approximations of the Theodorsen function

	Initial conditions			Converged approximation		
Case[a]	a	b	J_0	a	b	J
1	−0.377	−0.2	0.132	−0.4542	−0.1660	0.0215
2	−0.377	−0.2	0.0881	−0.4027	−0.1297	0.0109
	−0.0833	−1.0		−0.1343	−1.2660	
3	−0.377	−0.2	0.0507	−0.1524	−0.0490	0.00102
	−0.167	−0.5		−0.2212	−0.2385	
	0.0833	−1.0		−0.1088	−0.3576	
4	−0.377	−0.2	0.0439	−0.1058	−0.0367	0.000420
	−0.111	−0.333		−0.2877	−0.1853	
	0.0555	−0.667		−0.000912	−0.5681	
	−0.0278	−1.0		−0.1002	−0.5914	
5	−0.377	−0.2	0.0343	−0.2919	−0.1038	0.00732
	−0.133	−0.250		−0.1167	−0.2270	
	0.0666	−0.5		−0.1060	−1.2649	
	−0.0333	−0.75		−0.0853	−1.6161	
	0.0167	−1.0		0.0899	−2.4435	
6	−0.377	−0.2	0.0254	−0.0491	−0.0769	0.00811
	−0.121	−0.167		−0.3354	−0.1292	
	0.0606	−0.333		0.0343	−0.1682	
	−0.0303	−0.5		−0.0268	−0.2452	
	0.0151	−0.667		−0.0303	−0.2948	
	−0.00757	−1.0		−0.1230	−1.1911	
7	−0.377	−0.2	0.0253	−0.2349	−0.02994	0.000415
	−0.127	−0.167		0.1331	−0.02614	
	0.0635	−0.333		−0.000027	−0.1807	
	−0.0317	−0.5		−0.2896	−0.1827	
	0.0159	−0.667		−0.000113	−0.5848	
	−0.00793	−0.833		−0.1026	−0.5856	
	−0.00397	−1.0		−0.000272	−0.5848	
8	−0.165	−0.0455	0.0126	−0.1644	−0.05187	0.00119
	−0.355	−0.300		−0.3173	−0.2819	
9	−0.187	−0.0594	0.00138	−0.1058	−0.0367	0.000420
	−0.236	−0.254		−0.2876	−0.1853	
	−0.0769	−0.652		−0.1011	−0.5912	
10	−0.358	−0.1	0.0044	−0.1644	−0.05187	0.00119
	0.142	−0.2		0.000012	−0.05187	
	−0.284	−0.4		−0.3173	−0.2819	
11	−0.2	−0.2	0.07135	−0.1644	−0.05187	0.00119
	−0.3	−0.1		−0.3173	−0.2819	
12	−0.1	−0.1	0.1200	−0.1615	−0.0510	0.00118
	−0.1	−0.3		−0.3110	−0.2772	
	−0.2	−0.5		−0.00902	−0.3688	
13	0.1	−0.5	0.00745	−0.1170	−0.04897	0.00118
	−0.2	−0.2		−0.0507	−0.06095	
	−0.2	−0.1		0.002445	−0.07344	
	−0.2	−0.6		−0.3165	−0.2824	

[a]Cases 1-7 used the automatic choice presented in Eqs. (13-15) for x_0. Case 8 used the Jones approximation[10] for x_0. Cases 9 and 10 used two of Dowell's best three-pole fits for x_0. Cases 11-13 used arbitrary choices for x_0.

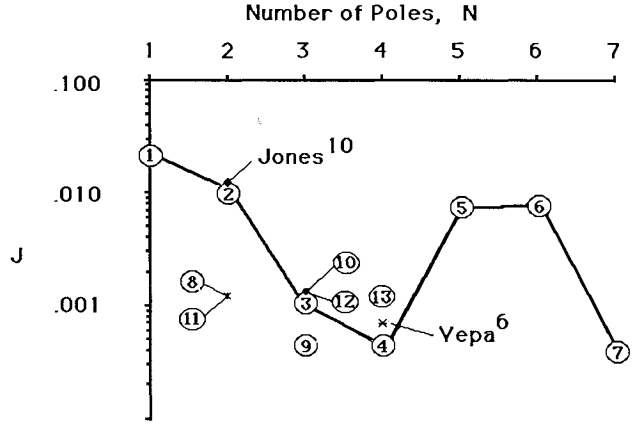

Fig. 2 Comparison of the square error in the approximations in Table 2 as a function of the order of the approximation. Also shown are the exponential time series approximation of Jones[10] and the Pade approximation of Vepa.[6]

with additional poles is not guaranteed and some judgment must be used in selecting the appropriate number.

Several of the 13 numerical cases of Table 2 compare the results obtained using the current procedure to well-known exponential series approximations. Case 1 uses as its starting point the most obvious single-pole approximation, with its pole chosen to match the maxima in $G(k)$ and its coefficient chosen to obtain the correct amplitude of $|G|$ at the maxima.[8] The converged solution in Fig. 3 shows almost an order-of-magnitude improvement in cost over the initial choice. Interestingly, although the choice of x_0 was based on the shape of G, the fit to the real part is substantially better than the fit to the imaginary part. Case 8 uses as its starting point the Jones approximation.[10] More than an order-of-magnitude improvement is made in the cost and the converged solution clearly tracks the actual Theodorsen function more closely than Jones' approximation in the reduced frequency span of interest (Fig. 4). Cases 9 and 10 start with the best third-order approximations of Dowell.[8] Both show substantial improvement. The best three-pole case found is

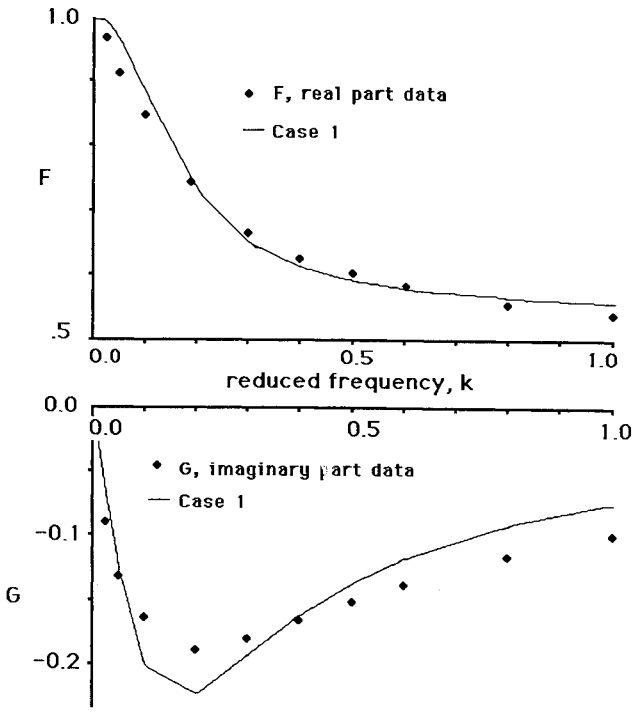

Fig. 3 Real and imaginary parts of the single-pole approximation in case 1.

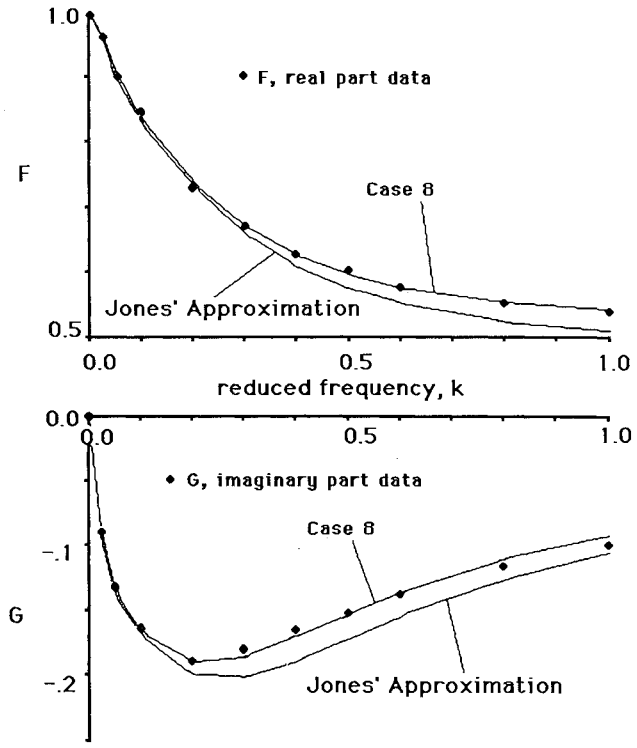

Fig. 4 Real and imaginary parts of the two-pole approximation in case 8, which was found using the Jones approximation as a starting point.

that of case 9, based upon Dowell's initial x_0. It is plotted in Fig. 5 and is nearly indistinguishable from the data. This three-pole fit is actually the best fit achieved by the current algorithm.

Having shown the dependence on the number of poles and improvement to traditional approximations, there remains the question of the uniqueness of the solution and its

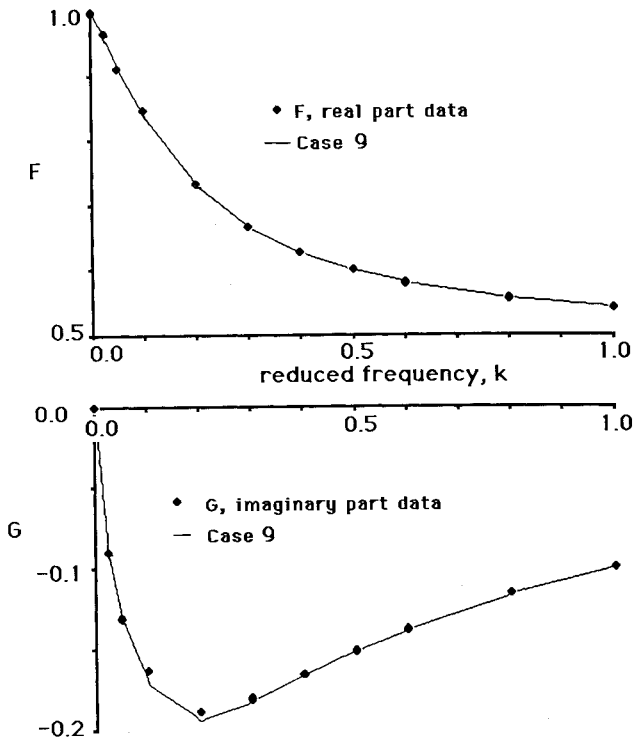

Fig. 5 Real and imaginary parts of the three-pole approximation in case 9. The approximation is nearly indistinguishable from the known values of F and G.

dependence on choice of starting condition x_0. To explore this, cases 11–13 were run with arbitrarily chosen initial conditions. In some instances, such as cases 8 and 11, different initial conditions converged to exactly the same answer. But when compared with case 2, another two-pole case with a dissimilar x_0, a different converged solution is obtained. Therefore, in the solution space of poles and coefficients, there exist local minima that are not global minima and a variety of initial conditions should be used to assure identification of a local minima close in value to the global minima.

Finally, an interesting effect can be noticed by carefully studying the converged solutions in Table 2. The optimization algorithm has the power to effectively turn off or eliminate a pole from the fit by driving its coefficient to zero. Comparison of cases 10 and 12, which started as three-pole examples with case 8, show that in each of the three-pole cases one pole has been so reduced in contribution that it has essentially become a two-pole fit. By comparison of the two poles at -0.06095 and -0.04897 in case 13 with the one pole at -0.05187 in case 8, one can see that, in other instances, two closely spaced poles effectively combine to mimic one single pole. Thus, two-pole cases 8 and 11, three-pole cases 10 and 12, and four-pole case 13 are in effect all the same two-pole approximation. Likewise, three-pole case 9, four-pole case 4, and seven-pole case 7 are all fundamentally the same. This can be best represented on Fig. 6, where the cost is plotted versus the number of effective poles in the fit. Note that there are still non-unique convergencies, and monotonically decreasing cost is not guaranteed. In summary, as with most optimizations, much more accurate answers can be found, but careful interpretation of the results are called for.

Comparison with a Pade Approximation

It is instructive to compare the exponential time series approximations for the Theodorsen circulation function C with

Table 3 Optimal approximations of the Theodorsen function in the range $0 \le k \le 1$ ($a^0 = 1$)

Order, N	a_i	b_i
1	−0.4542	−0.1660
2	−0.1644	−0.05187
	−0.3173	−0.2819
3	−0.1058	−0.0367
	−0.2876	−0.1853
	−0.1011	−0.5912

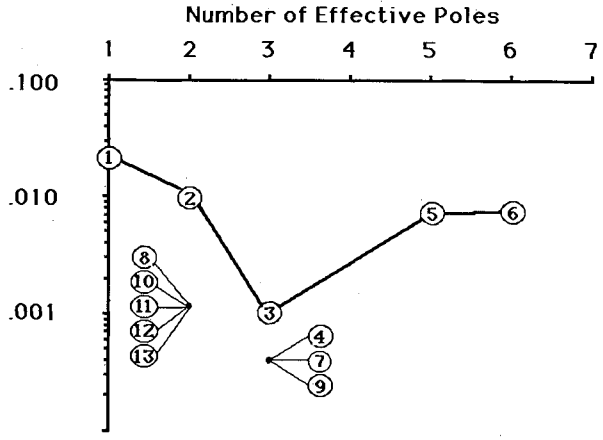

Fig. 6 Comparison of the square error in the approximation of Table 2 as a function of the effective order of the approximation.

the Pade approximation of Vepa,[6] which in the Laplace domain is

$$C(s) = \frac{s^4 + 0.761036s^3 + 0.102058s^2 + 0.00255067s}{2s^4 + 1.063939s^3 + 0.113938s^2 + 0.0261680s} \frac{+9.55732\times 10^{-6}}{+9.55732\times 10^{-6}}$$

When the Laplace domain variable s is set to ik, the corresponding approximations for F' and G' can be calculated. For comparison with the above approximations, the square error J is formulated for this approximation using uniform weighting vectors as before and is found to be 6.82×10^{-4}, which has been plotted in Fig. 2. Table 2 shows that case 9, a third-order approximation found using one of Dowell's[8] approximations as a starting point, has a cost of 4.2×10^{-4}. Therefore, the fourth-order Pade approximation is slightly less accurate than an optimized third-order exponential time series approximation found using the procedure presented in this paper.

Conclusion

An algorithm has been presented for the approximate representation of unsteady aerodynamic operators as finite-order exponential time series. The approximation is achieved by numerically minimizing the weighted square error between the approximate representation and known values of the aerodynamic operator in the frequency domain with both the coefficients and poles treated as free parameters. The parameter search is constrained to consider only poles that lie in the left half-plane.

By including the poles as free parameters in the fit, significantly better one-, two-, and three-pole approximations to the Theodorsen function were found than are commonly in use. These are summarized in Table 3. It was concluded that a two- or certainly three-pole fit is adequate and no advantage is obtained from higher-order fits. In addition, a three-pole fit was found to be more optimal than a fourth-order Pade approximation in the frequency range of study. This fact and the fact that the poles or states of the aerodynamic transfer function are readily extractable from the exponential time series indicate that this method is more useful in aeroelastic analysis.

As with all nonlinear optimizations, some care must be made in interpreting the results. The accuracy of the fit was not found to improve monotonically with an increasing number of poles. The converged minima was not necessarily the global minima and is dependent on the initial approximation vector x_0. Finally, the optimization has the power to effectively reduce the number of active poles in the fit, often driving a higher-order fit to a minima found for a lower number of poles. But with judgment in interpreting results, superior exponential time series approximations can be obtained by this method.

Acknowledgments

This paper is an extension of work reported in Ref. 5, which resulted from work done at Hughes Aircraft Company, Radar Systems Group, as part of the Massachusetts Institute of Technology Engineering Internship Program.

References

[1]Bisplinghoff, R.L., Ashley, J., and Halfman, R.L., *Aeroelasticity,* Addison-Wesley, Reading, MA, 1955.

[2]Edwards, J.E., Ashley, H., and Breakwell, J.V., "Unsteady Aerodynamic Modeling for Arbitrary Motions," *AIAA Journal,* Vol. 17, April 1979, pp. 365–374.

[3]Dugungii, J. and Bundas, D.J., "Flutter and Forced Response of Mistuned Rotors Using Standing Wave Analysis," *AIAA Journal,* Vol. 22, Nov. 1984, pp. 1652–1661.

[4]Crawley, E.F., "Aeroelastic Formulations for Turbomachines and Propellers," *Proceedings of Fourth International Symposium on Unsteady Aerodynamics in Turbomachines and Propellers,* Cambridge University Press, London, Sept. 1984.

[5]Peterson, L.D., "Simulation of an Aircraft's Rigid Dynamic and Aeroelastic Response for Evaluation of Radar Motion Compensation Techniques," Master of Science Thesis, Massachusetts Institute of Technology, Cambridge, 1983.

[6]Vepa, R., "On the Use of Pade Approximants to Represent Unsteady Aerodynamic Loads for Arbitrary Small Motions of Wings," AIAA Paper 76-17, Jan. 1976.

[7]Dunn, H.J., "An Analytical Technique for Approximating Unsteady Aerodynamics in the Time Domain," NASA TP 1738, 1980.

[8]Dowell, E.H., "A Simple Method for Converting Frequency Domain Aerodynamics to the Time Domain," NASA TM-81844, 1980.

[9]Theodorsen, T., "General Theory of Aerodynamic Instability and the Mechanism of Flutter," NACA Rept. 496, 1934.

[10]Jones, R.T., "The Unsteady Lift of a Wing of Finite Aspect Ratio," NACA Rept. 681, 1940.

[11]Desmarais, R.N., "A Continued Fraction Representation for Theodorsen's Circulation Function," NASA TM-81838, 1980.

[12]Thomas, G.B., *Calculus and Analytic Geometry,* Addison-Wesley, Reading, MA, 1968.